SCIENTIFIC REPORTS
nature research

Check for updates

OPEN

Increased O-GlcNAcylation rapidly decreases $GABA_AR$ currents in hippocampus but depresses neuronal output

L. T. Stewart[1,3], K. Abiraman[1,3], J. C. Chatham[2] & L. L. McMahon[1] ✉

O-GlcNAcylation, a post-translational modification involving O-linkage of β-*N*-acetylglucosamine to Ser/Thr residues on target proteins, is increasingly recognized as a critical regulator of synaptic function. Enzymes that catalyze O-GlcNAcylation are found at both presynaptic and postsynaptic sites, and O-GlcNAcylated proteins localize to synaptosomes. An acute increase in O-GlcNAcylation can affect neuronal communication by inducing long-term depression (LTD) of excitatory transmission at hippocampal CA3-CA1 synapses, as well as suppressing hyperexcitable circuits *in vitro* and *in vivo*. Despite these findings, to date, no studies have directly examined how O-GlcNAcylation modulates the efficacy of inhibitory neurotransmission. Here we show an acute increase in O-GlcNAc dampens GABAergic currents onto principal cells in rodent hippocampus likely through a postsynaptic mechanism, and has a variable effect on the excitation/inhibition balance. The overall effect of increased O-GlcNAc is reduced synaptically-driven spike probability via synaptic depression and decreased intrinsic excitability. Our results position O-GlcNAcylation as a novel regulator of the overall excitation/inhibition balance and neuronal output.

Synaptic integration and spike initiation in neurons is controlled by synaptic inhibition, which strongly influences neuronal output and information processing[1]. Importantly, the balance of excitation to inhibition (E/I) is crucial to the proper functioning of circuits, and E/I imbalances have been implicated in a number of neurodevelopmental disorders and neurodegenerative diseases including schizophrenia, autism spectrum disorders, and Alzheimer's disease[2–5]. Thus, understanding the mechanisms that modulate the strength of inhibitory transmission is fundamental to unraveling how neuronal circuits function in normal and disease states.

Fast inhibitory transmission in the central nervous system is mediated by $GABA_A$ receptors ($GABA_ARs$), which are pentameric ligand-gated ion channels. The strength of this inhibition can be rapidly up- or down-regulated by post-translational modifications including ubiquitination[6], palmitoylation[7,8], and phosphorylation[9] of $GABA_AR$ subunits and/or associated proteins, which can alter channel function, trafficking, or stability at the membrane. While there is a vast body of literature on these post-translational modifications, O-GlcNAcylation, involving the O-linkage of β-*N*-acetylglucosamine (O-GlcNAc) to Ser/Thr residues on target proteins, remains severely understudied, with no examination to date of the effect of protein O-GlcNAcylation on inhibitory synapse physiology.

Addition and removal of O-GlcNAc are catalyzed by the single pair of enzymes O-GlcNAc transferase (OGT) and O-GlcNAcase (OGA). O-GlcNAcylation is essential, as genetic deletion of OGT and OGA are lethal[10,11]. O-GlcNAcylation is metabolically-regulated and highly dynamic; global changes reversibly occur within minutes, and are dictated by availability of UDP-GlcNAc, which is synthesized from glucose via the hexosamine biosynthetic pathway (HBP)[12]. The brain contains the second highest level of O-GlcNAcylated proteins in the body[13], with the hippocampus expressing one of the highest levels of OGT/OGA[14]. Notably, the majority of O-GlcNAcylated proteins are found at the synapse[15]. However, only a handful of studies have examined the functional impact of O-GlcNAcylation in the brain[16–21].

[1]Department of Cell, Developmental and Integrative Biology, University of Alabama at Birmingham, Birmingham, AL, 35294, USA. [2]Department of Pathology, University of Alabama at Birmingham, Birmingham, AL, 35294, USA. [3]These authors contributed equally: L. T. Stewart and K. Abiraman. ✉e-mail: mcmahon@uab.edu

Previous work from our lab has examined the role of protein O-GlcNAcylation at glutamatergic synapses in hippocampal area CA1, where O-GlcNAcylation of the AMPA receptor (AMPAR) GluA2 subunit initiates long-term synaptic depression, termed 'O-GlcNAc LTD'[19]. Recent work[22] showing that increased O-GlcNAc suppresses excitatory transmission at CA3-CA1 synapses through the removal of GluA2 containing AMPARs is consistent with our findings. Additionally, increased O-GlcNAcylation dampens picrotoxin-induced epileptiform activity in area CA1 and CA3, and reduces seizure activity in the pentylenetetrazole *in vivo* model of seizure activity in mice[18]. Deletion of OGT in αCaMKII expressing neurons in the adult rodent brain causes a reduction in excitatory synaptic input onto hypothalamic PVN neurons[23], while OGT knock-out (KO) specifically from hypothalamic AgRP neurons reduces excitability via its effect on voltage-gated potassium channels[17]. Conversely, no studies to date have examined the role of protein O-GlcNAcylation in modulating inhibitory synaptic function. Because serine phosphorylation of $GABA_AR$ subunits regulates the efficacy of neuronal inhibition[24,25], it is highly likely that serine O-GlcNAcylation will also control $GABA_AR$ function and neuronal inhibition.

Here, we show that an acute increase in protein O-GlcNAcylation rapidly induces a long-lasting decrease in strength of GABAergic synaptic transmission in hippocampus that is likely through an effect on post-synaptic $GABA_ARs$. This depression of inhibition produces a variable effect on the excitation/inhibition ratio in individual pyramidal cells, likely due to a simultaneous depression at excitatory synapses. However, the net effect in the intact circuit is a depression of neuronal output due to a simultaneous decrease in intrinsic excitability together with reduced synaptic drive at both excitatory and inhibitory synapses. Thus, global changes in O-GlcNAcylation induce complex changes in network activity by targeting excitatory and inhibitory synapses together with direct effects on intrinsic excitability.

Results

Acute increase in protein O-GlcNAcylation depresses GABAergic transmission onto CA1 pyramidal cells and dentate granule cells. To determine if protein O-GlcNAcylation modulates $GABA_AR$-mediated inhibitory neurotransmission, we used whole-cell voltage clamp to record spontaneous inhibitory post-synaptic currents (sIPSCs) from CA1 pyramidal cells while blocking glutamatergic transmission using DNQX (10 μM) and DL-AP5 (50 μM). Following a 5 min baseline, we bath applied the HBP substrate glucosamine (GlcN, 5 mM) and the OGA inhibitor thiamet-G (TMG, 1μM) to acutely increase protein O-GlcNAc levels, as done previously[18,19] (Fig. 1Ai). We found a significant reduction in sIPSC amplitude (Fig. 1Aii, cumulative probability distribution, $p < 0.0001$, KS D value = 0.217, Kolmogorov-Smirnov test; inset: $p < 0.0001$, Wilcoxon matched-pairs signed rank test) and inter-event interval (Fig. 1Aiii, cumulative probability distribution, $p < 0.0001$, KS D value = 0.084, Kolmogorov-Smirnov test; inset: $p < 0.0001$, Wilcoxon matched-pairs signed rank test) in CA1 pyramidal cells. To ensure that the change in amplitude and inter-event interval of the sIPSCs was not a consequence of a technical artifact, sIPSCs during baseline and 5 min after GlcN + TMG application were averaged and scaled (Fig. 1Aii,Bii, inset); the traces perfectly overlapped, indicating that the decrease in sIPSC amplitude and frequency observed are not due to an increase in series resistance caused by prolonged recording or by washing on GlcN + TMG. It is also important to note that we observed a shift in holding current following application of GlcN + TMG (baseline: -138.2 ± 13.6 pA vs. GlcN + TMG: -106.4 ± 11.5 pA, n = 9 cells, 5 rats, $p = 0.006$, paired t-test), suggesting possible modulation of extrasynaptic $GABA_ARs$, which will be investigated in future experiments.

In order to determine if this decrease in sIPSCs induced by GlcN + TMG is specific to CA1 pyramidal cells or if it occurs at inhibitory synapses on other cells, we recorded sIPSCs from dentate gyrus granule cells (GCs) before and after bath application of GlcN + TMG (Fig. 1Bi). We observed the same effect, namely a decrease in sIPSC amplitude (Fig. 1Bii, cumulative probability distribution, $p < 0.0001$, KS D value = 0.11, Kolmogorov-Smirnov test; inset: $p < 0.0001$, Wilcoxon matched-pairs signed rank test) and increase in inter-event interval (Fig. 1Biii, cumulative probability distribution, $p < 0.0001$, KS D value = 0.055, Kolmogorov-Smirnov test; inset: $p < 0.0001$, Wilcoxon matched-pairs signed rank test), but no shift in holding current ($p = 0.768$, paired t-test). These findings suggest that O-GlcNAc-mediated depression of GABAergic transmission is likely to be a general mechanism occurring at many inhibitory synapses in the brain.

The decrease in sIPSCs following increased O-GlcNAcylation could arise from a decrease in presynaptic GABA release, or from decreased postsynaptic $GABA_AR$ function. To distinguish between these possibilities, we recorded mIPSCs from both CA1 pyramidal cells and GCs in the presence of the voltage-gated sodium channel blocker TTX (1 μM) (Fig. 2Ai,Bi). A change in mIPSC frequency typically reflects a change in presynaptic neurotransmitter release probability, while a change in mIPSC amplitude indicates a change in postsynaptic receptor function. Bath application of GlcN + TMG resulted in a reduction in mIPSC amplitude (Fig. 2Aii, cumulative probability distribution, $p < 0.0001$, KS D value = 0.24, Kolmogorov-Smirnov test; inset: $p < 0.0001$, Wilcoxon matched-pairs signed rank test), but not inter-event interval (Fig. 2Aiii, cumulative probability distribution, $p = 0.96$, KS D value = 0.032, Kolmogorov-Smirnov test; inset: $p < 0.0001$, Wilcoxon matched-pairs signed rank test) in CA1 pyramidal cells. We observed a similar decrease in mIPSC amplitude in dentate GCs (Fig. 2Bii, cumulative probability distribution, $p < 0.0001$, KS D value = 0.12, Kolmogorov-Smirnov test; inset: $p < 0.0001$, Wilcoxon matched-pairs signed rank test), but in contrast to CA1, we also observe a slight but significant increase in mISPC inter-event interval (Fig. 2Biii, cumulative probability distribution, $p < 0.0001$, KS D value = 0.099, Kolmogorov-Smirnov test; inset: $p < 0.0001$, Wilcoxon matched-pairs signed rank test). However, the very small difference in mean values between control (373.5 ± 7.3 ms) and GlcN + TMG (374.1 ± 7.4 ms) suggests this significant difference may not be biologically relevant. Collectively, the decrease in mIPSC amplitude in the absence of a decrease in inter-event interval, at least in CA1 pyramical cells, is consistent with the interpretation that the dampening of inhibitory transmission following increased O-GlcNAcylation is due to a reduction in postsynaptic $GABA_AR$ function.

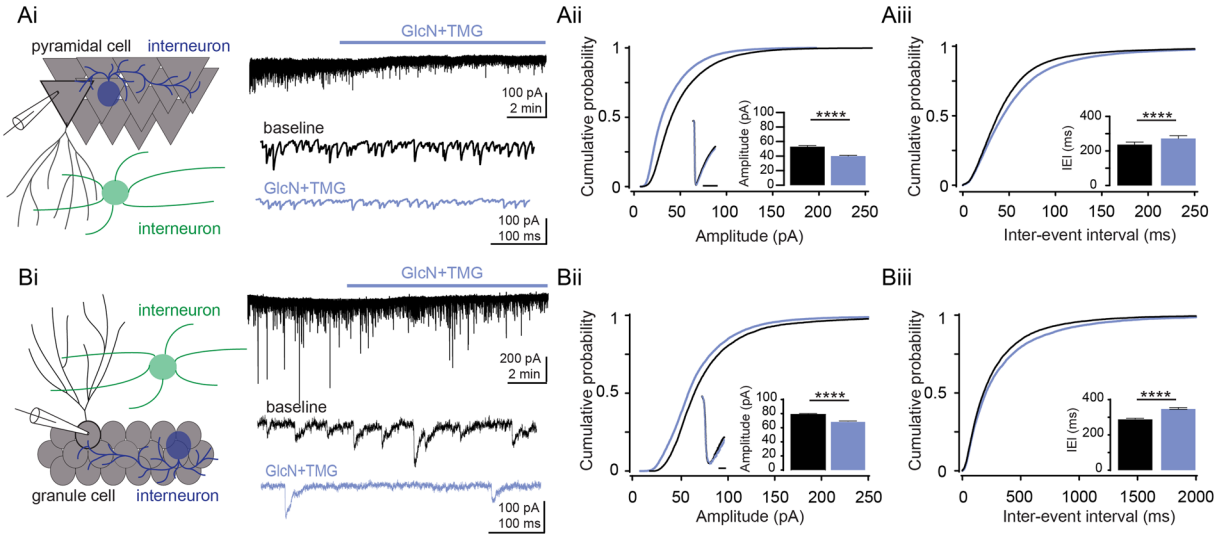

Figure 1. Acute increase in O-GlcNAcylation reduces spontaneous IPSCs in hippocampal principal cells. **(Ai)** (left) Schematic depicting recording set up in CA1. (right) representative sIPSC trace from a CA1 pyramidal cell showing (top) GlcN + TMG wash on and (bottom) expanded time scale (control (black) and GlcN + TMG (blue)). **(Aii)** Cumulative probability distribution of sIPSC amplitude ($p < 0.0001$, KS D value = 0.2, Kolmogorov-Smirnov test); *inset:* (left) scaled average sIPSC trace before (black) and after (blue) GlcN + TMG, scale bar: 5 ms. (right) average (±SEM) sIPSC amplitude. Baseline: 43.1 ± 0.5pA, GlcN + TMG: 31.4 ± 0.4 pA ($p < 0.0001$, Wilcoxon matched-pairs signed rank test, n = 9 cells, 5 rats).Inset shows no change in the rise-time or decay of averaged and scaled sIPSCs from before and after GlcN + TMG exposure. **(Aiii)** Cumulative probability distribution of sIPSC IEI $p < 0.0001$, KS D value = 0.084, Kolmogorov-Smirnov test; *inset:* average (± SEM) sIPSC inter-event interval (IEI). Baseline: 53.1 ± 0.9 ms, GlcN + TMG: 62.4 ± 1.2 ms ($p < 0.0001$, Wilcoxon matched-pairs signed rank test, n = 9 cells, 5 rats). **(Bi)** (left) Schematic depicting recording set up in dentate gyrus and (right) representative sIPSC trace from a granule cell showing (top) GlcN + TMG wash on and (bottom) expanded time scale. **(Bii)** Cumulative probability distribution of sIPSC amplitude ($p < 0.0001$, KS D value = 0.11, Kolmogorov-Smirnov test); *inset:* (left) scaled average sIPSC trace before (black) and after (blue) GlcN + TMG, scale bar: 5 ms. (right) average (± SEM) sIPSC amplitude. Baseline: 78.9 ± 0.6 pA, GlcN + TMG: 69.1 ± 0.5 pA ($p < 0.0001$, Wilcoxon matched-pairs signed rank test, n = 11 cells, 7 rats).).Inset shows no change in the rise-time or decay of averaged and scaled sIPSCs from before and after GlcN + TMG exposure. **(Biii)** Cumulative probability distribution of sIPSC IEI; *inset:* average (±SEM) sIPSC IEI ($p < 0.0001$, KS D value = 0.055, Kolmogorov-Smirnov test). Baseline: 301.4 ± 3.6 ms, GlcN + TMG: 349.5 ± 4.7 ms ($p < 0.0001$, Wilcoxon matched-pairs signed rank test, n = 11 cells, 7 rats). ****$p < 0.0001$.

O-GlcNAcylation induces long-term depression of inhibitory transmission. We next tested if O-GlcNAcylation similarly affects the amplitude of electrically evoked IPSCs (eIPSCs), as evoked transmission may be dependent upon presynaptic vesicle pools (reviewed in[26]) distinct from those involved in spontaneous release. To address this and remaining questions, we focused our experiments on CA1 pyramidal cells. Following a 5 min stable baseline of eIPSCs (Cs Gluconate pipet solution; $E_{Cl^-} = -50$ mV), bath applied GlcN + TMG elicited a significant reduction in eIPSC amplitude that lasted the duration of the recording (Fig. 3Ai,Aiii, $p = 0.001$, paired t-test), with no change in decay kinetics (Fig. 3Aii, $p = 0.23$, paired t-test).

We previously reported that a 10 min exposure to GlcN (5 mM) alone induces a significant increase in O-GlcNAcylation in hippocampus that is readily reversed within a 10 min washout, while O-GlcNAcylation remains elevated for up to 2 hrs following a 10 min exposure to TMG[19]. Importantly, the depression of transmission at CA3-CA1 synapses induced by GlcN outlasted the transient increase in protein O-GlcNAcylation, demonstrating expression of a long-term depression (LTD) at these synapses[19]. To test if O-GlcNAcylation similarly causes long-term depression at GABAergic synapses onto CA1 pyramidal cells, we applied GlcN alone for 10 min and recorded eIPSCs for 10 min during washout and observed a persistent reduction in amplitude (Fig. 3Bi,Biii, $p = 0.003$, paired t-test), consistent with expression of a form of LTD at GABAergic synapses.

O-GlcNAcylation has a variable effect on the E/I ratio. Since O-GlcNAcylation induces LTD of both excitatory[19] and inhibitory transmission onto CA1 pyramidal cells (Fig. 3), we wondered what the overall effect of increased O-GlcNAc is on the balance of excitation to inhibition (E/I). Thus, we measured the E/I ratio at CA3-CA1 synapses by recording compound synaptic currents consisting of mono-synaptic EPSCs followed by di-synaptic IPSCs in whole-cell recordings of CA1 pyramidal cells voltage-clamped at −30 mV. We observed a linear trend in the balance of E to I, with the E/I ratio increasing following GlcN + TMG application (Fig. 4Ai, $p < 0.0001$, repeated measures one-way ANOVA with post hoc test for linear trend). However, at the single cell level, the change in the E/I ratio was variable with just over half of cells (n = 6/10) displaying a statistically

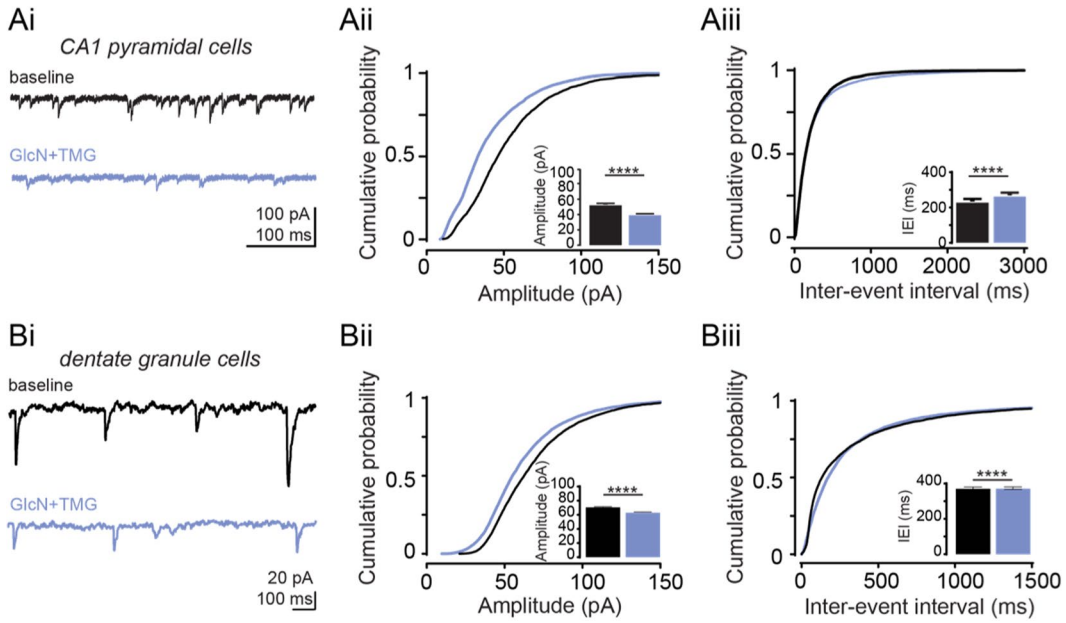

Figure 2. Acute increase in O-GlcNAcylation reduces miniature IPSC amplitude in hippocampal principal cells. **(Ai)** Representative mIPSC trace from CA1 pyramidal cell before (black) and after (blue) GlcN + TMG. **(Aii)** cumulative probability distribution of mIPSC amplitude ($p < 0.0001$, KS D value = 0.24, Kolmogorov-Smirnov test); *inset:* average (± SEM) mIPSC amplitude. Baseline: 53.0 ± 1.6 pA, GlcN + TMG: 40.0 ± 1.0 pA ($p < 0.0001$, Wilcoxon matched-pairs signed rank test, n = 7 cells, 5 rats). **(Aiii)** Cumulative probability distribution of mIPSC IEI ($p = 0.96$, KS D value = 0.03, Kolmogorov-Smirnov test); *inset:* average (± SEM) mIPSC IEI. Baseline: 236.7 ± 14.3 ms vs GlcN + TMG: 271.5 ± 16.2 ms ($p < 0.0001$, Wilcoxon matched-pairs signed rank test, n = 7 cells, 5 rats). **(Bi)** Representative mIPSC trace from dentate granule cell before (black) and after (blue) GlcN + TMG. **(Bii)** Cumulative probability distribution of mIPSC amplitude ($p < 0.0001$, KS D value = 0.1, Kolmogorov-Smirnov test); *inset:* average (±SEM) mIPSC amplitude. Baseline: 71.1 ± 0.4pA vs GlcN + TMG: 63.3 ± 0.4 pA ($p < 0.0001$, Wilcoxon matched-pairs signed rank test, n = 12 cells, 6 rats). **(Biii)** Cumulative probability distribution of mIPSC IEI ($p < 0.0001$, KS D value = 0.099, Kolmogorov-Smirnov test); *inset:* average (±SEM) mIPSC IEI. Baseline: 373.5 ± 7.4 ms, GlcN + TMG: 368.8 ± 7.5 ms ($p = 0.0005$, Wilcoxon matched-pairs signed rank test, n = 12 cells, 6 rats). ****$p < 0.0001$.

increased ratio following GlcN + TMG exposure ($p \leq 0.009$, paired t-test on each individual cell comparing 5 mins before and 5 min following 5 min exposure to GlcN + TMG), and a statistically decreased E/I ratio in the rest (n = 4/10; $p \leq 0.01$, paired t-test on each individual cell comparing 5 mins before and 5 min following 5 min exposure to GlcN + TMG). Thus, comparing the mean E/I ratios before and after GlcN + TMG exposure when all cells were averaged yields no significant difference (Fig. 4Aii, $p = 0.08$, paired t-test; red circles and blue circles indicate increased and decreased E/I respectively).

We next examined the compound EPSCs and IPSCs individually as both can be depressed by inceased O-GlcNAc. GlcN + TMG application caused a significant reduction in the IPSC component of the compound current (Fig. 4Bi–Biii, open circles shown as %baseline current, paired t-test, $p = 0.03$), with no significant change in the EPSC component (Fig. 4Bi–Biii, closed circles shown as % baseline current, $p = 0.43$, Wilcoxon matched-pairs signed rank test). These data indicate that on average, increasing O-GlcNAc elicits a greater depression of the disynaptic $GABA_AR$-mediated IPSC than the mono-synaptic glutamatergic EPSC. Normally, $GABA_AR$-mediated transmission limits the amplitude of EPCSs through shunting the excitatory potential, and when the inhibitory shunt is decreased or blocked, the EPSC amplitude increases. Thus, decreasing the inhibitory shunt via the O-GlcNAc-mediated decrease in IPSC amplitude predicts that the EPSC amplitude should increase[27], which we observed in a fraction of the cells (n = 4/10, Fig. 4Aiii). On the other hand, the GluA2-AMPAR mediated O-GlcNAc LTD at CA3-CA1 synapses[19], occurring in parallel with the decrease in IPSC amplitude could occlude the expected increase in EPSC amplitude cause by the decreased inhibitory shunt, which we observed in the majority of our cells (n = 6/10, Fig. 4Aiii). Thus, the overall effect of increasing O-GlcNAc is extremely complicated given that exposure to GlcN + TMG causes synaptic depression at both glutamatergic and GABAergic synapses within minutes, and the impact on the E/I ratio will be driven by the magnitude of the change in the EPSC vs IPSC, with increases in the E/I ratio being driven by a larger increase in the EPSC or smaller decrease in the EPSC amplitude compared to the IPSC (compare blue and red circles in Fig. 4Aiii). We also confirmed this variable effect on the E/I ratio in current clamp recordings from CA1 pyramidal cells, and found, once again, a linear trend for an increase in the E/I ratio (Fig. 4Ci, $p < 0.01$, repeated measures one-way ANOVA with post hoc test for linear trend) following GlcN + TMG exposure, and a greater depression of the IPSP vs EPSP (Fig. 4Di–Diii, IPSP vs EPSP: $p = 0.01$ and $p = 0.4$, paired t-test) translating into an increase in the E/I ratio in the majority of

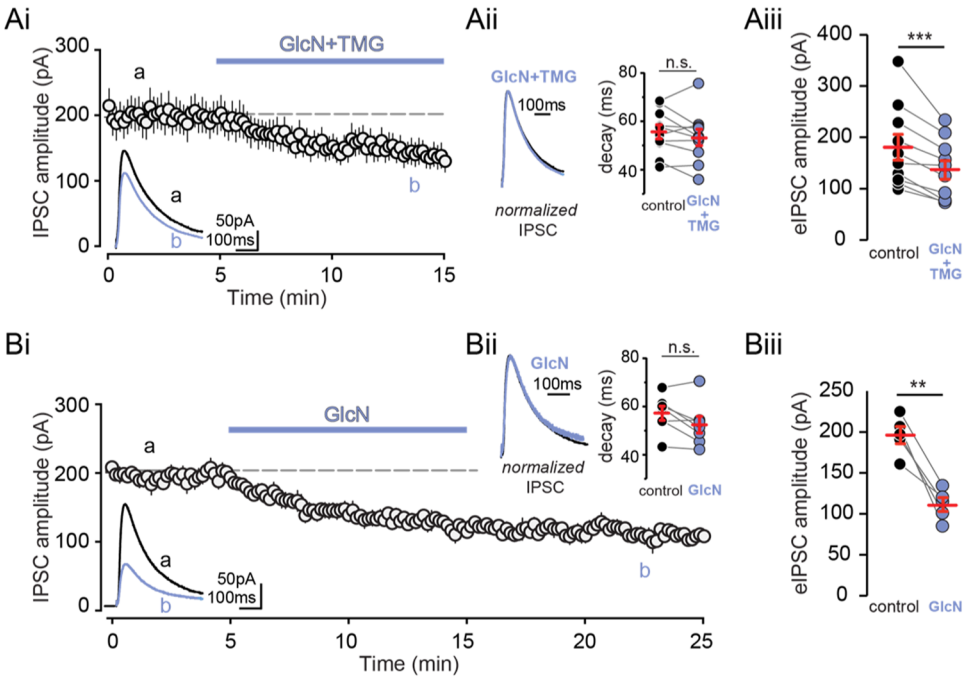

Figure 3. Increasing O-GlcNAcylation reduces evoked IPSC amplitude in CA1 pyramidal cells. **(Ai)** Group data showing average (±SEM) evoked IPSC (eIPSC) amplitude in control conditions and following GlcN + TMG wash on. *Inset:* representative eIPSC traces before (black) and after GlcN + TMG (blue). **(Aii)** (left) Normalized representative eIPSC traces and (right) decay time before (black) and after GlcN + TMG (blue). Red horizontal bars represent the mean ± SEM. control: 55.7 ± 2.9 ms vs GlcN + TMG: 53.4 ± 3.4 ms ($p = 0.23$, paired-test, n = 10 cells, 5 rats). **(Aiii)** eIPSC amplitudes before (black) and after (blue) GlcN + TMG. Red horizontal bars represent the mean ± SEM. control: 180.9 ± 25.1 pA vs GlcN + TMG 136.7 ± 18.3pA ($p = 0.001$, paired-test, n = 10 cells, 5 rats). **(Bi)** Group data showing average (±SEM) evoked IPSC amplitude in control conditions and following GlcN wash on and wash out. *Inset:* representative eIPSC traces before (black) and after GlcN (blue) wash out. **(Bii)** (left) Normalized representative eIPSC traces and (right) decay time before (black) and after (blue) GlcN wash out. Red horizontal bars represent the mean ± SEM. control: 57.1 ± 2.9 ms vs GlcN: 52.4 ± 3.5 ms. ($p = 0.06$, paired-test, n = 5 cells, 2 rats). **(Biii)** eIPSC amplitudes before (black) and after (blue) GlcN wash out. Red horizontal bars represent the mean ± SEM. control: 196.3 ± 10.5 pA vs GlcN + TMG 111.4 ± 8.4 pA ($p = 0.003$, paired-test, n = 5 cells, 2 rats). **$p < 0.01$,****$p < 0.001$.

cells (Fig. 4Cii, n = 4/6 cells, $p \leq 0.01$, paired t-test on each individual cell comparing 5 mins before and 5 min following 5 min exposure to GlcN + TMG).

O-GlcNAcylation reduces action potential probability in CA1 pyramidal cells. How does this variable effect of increased O-GlcNAc on the E/I ratio affect neuronal output? In a previous study, we reported that increasing O-GlcNAc decreased basal spontaneous activity of CA3 pyramidal cells in an intact circuit, and depressed epileptic activity in area CA1 in hyperexcitable conditions generated by blocking $GABA_A$Rs[18]. Therefore, to determine the net effect of increasing protein O-GlcNAcylation on CA1 pyramidal cell output when the circuit is intact, we carried out current-clamp recordings from CA1 pyramidal cells and measured synaptically driven AP probability before and after application of GlcN + TMG. Stimulus intensity was set to achieve a ~25–50% success rate of generating a synaptically driven AP during the 5 min baseline (Fig. 5Ai, 0–5 min) after which GlcN + TMG were bath applied to increase O-GlcNAc levels (Fig. 5Ai, 5–20 min). Increasing O-GlcNAcylation caused a significant reduction in AP probability in all recorded cells, despite the increase in E/I ratio (Fig. 5Aii,Aiii, $p < 0.0001$, paired t-test). Importantly, control experiments were interleaved to rule out technical artifacts since AP probability is particularly sensitive to any change in the quality of the recording (Fig. 5Bi-Biii, $p = 0.56$, paired t-test).

As a further test of the effects of increasing O-GlcNAcylation on the net activity in the intact circuit, we performed a complementary experiment measuring the output of the CA1 population by recording extracellular population spikes (pSpike) in the CA1 pyramidal cell layer during a 10 min application of GlcN + TMG (Fig. 5Ci, 10–15 min). Consistent with the single-cell recordings, we observed a significant and sustained reduction in pSpike amplitude following an increase in O-GlcNAcylation (Fig. 5Cii, $p = 0.004$, paired t-test), which supports our previous report of decreased CA3 output in the context of increased protein O-GlcNAcylation[18].

Reduced intrinsic excitability of CA1 pyramidal cells contributes to the O-GlcNAc-mediated depression of excitability. The decrease in synaptically-evoked AP probability following increased O-GlcNAcylation may arise as a consequence of non-mutually exclusive synaptic and intrinsic mechanisms.

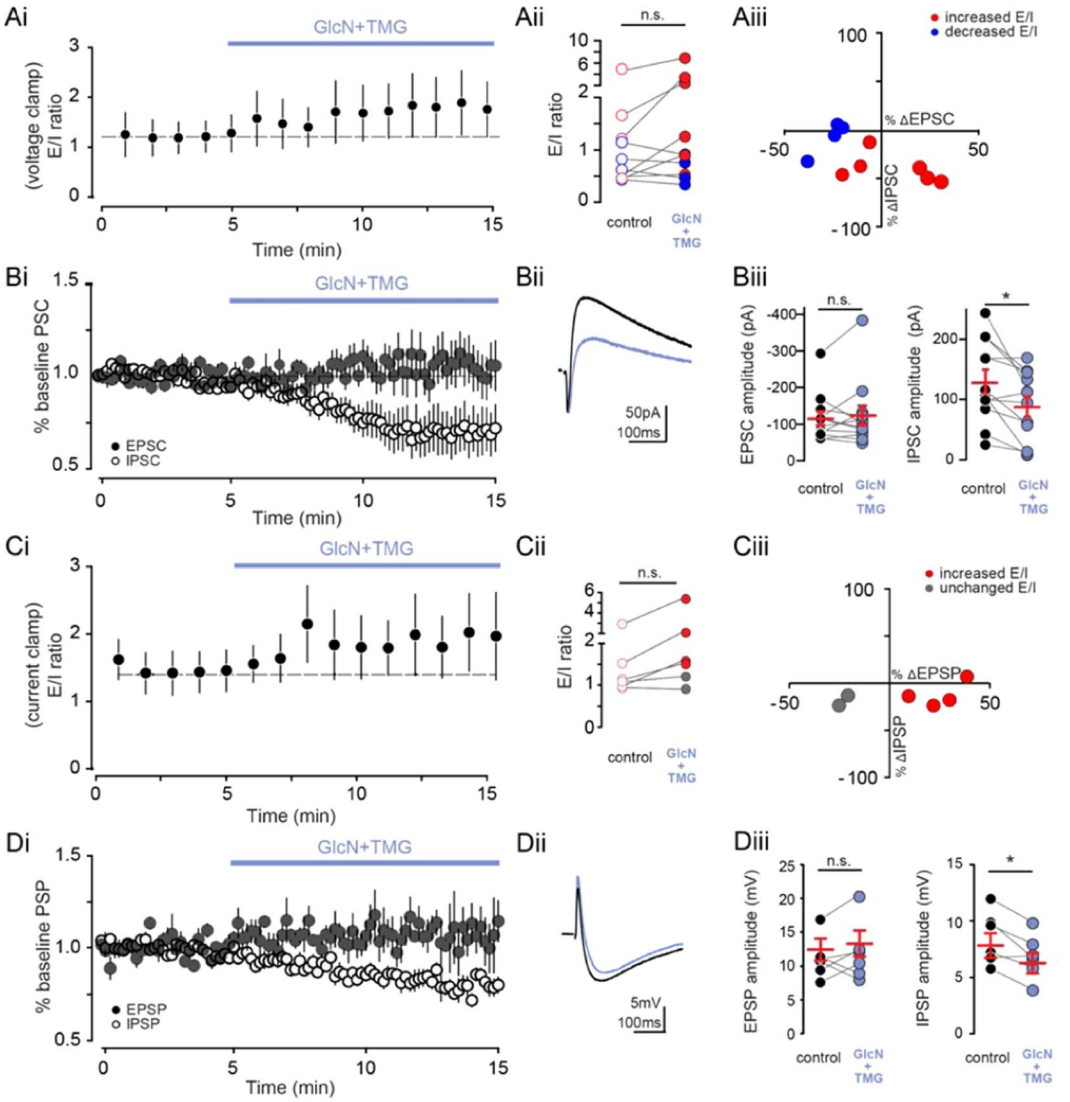

Figure 4. Increasing O-GlcNAcylation has a variable effect on E- I ratio in pyramidal cells. **(Ai)** Group data showing average (±SEM) E/I ratio using voltage clamp in control conditions and following GlcN + TMG wash on ($p < 0.0001$, repeated measures one-way ANOVA and post hoc test for linear trend, n = 10 cells, 4 rats). **(Aii)** E/I ratio before (open circles) and after (filled circles) GlcN + TMG. control: 1.2 ± 0.4 vs GlcN + TMG: 1.8 ± 0.6 ($p = 0.08$, paired t-test, n = 10 cells, 4 rats). Red circles indicate increased E/I and blue circles indicate decreased E/I ratio. **(Aiii)** Relationship between percent change in the EPSC and IPSC following GlcN + TMG from the recordings in Ai. Red circles indicate increased E/I and blue circles indicate decreased E/I ratio. **(Bi)** Normalized group data showing average (±SEM) evoked mono-synaptic EPSC (filled circles) and di-synaptic IPSC (open circles) amplitude in control conditions and following GlcN + TMG wash on. **(Bii)** Representative compound EPSC and IPSC before (black) and after (blue) GlcN + TMG. **(Biii)** EPSC amplitude before (black) and after (blue) GlcN + TMG. Red horizontal bars represent the mean ± SEM. control: −120.2 ± 22.1 pA vs GlcN + TMG: −116.1 ± 30.7 pA ($p = 0.43$, Wilcoxon matched-pairs signed rank test, n = 10 cells, 4 rats). (right) IPSC amplitude before (black) and after (blue) GlcN + TMG. Red horizontal bars represent the mean ± SEM. control: 130.2 ± 19.5 pA vs GlcN + TMG: 88.7 ± 16.6 pA ($p = 0.03$, paired t-test, n = 10 cells, 4 rats). **(Ci)** Group data showing average (±SEM) E/I ratio using current clamp in control conditions and following GlcN + TMG wash on ($p < 0.01$, repeated measures one-way ANOVA and post hoc test for linear trend, n = 6 cells, 3 rats). **(Cii)** E/I ratio before (open circles) and after (filled circles) GlcN + TMG. control: 1.4 ± 0.3 vs GlcN + TMG: 2.1 ± 0.7 ($p = 0.1$, paired t-test, n = 6 cells, 3 rats). Red circles indicate increased E/I and blue circles indicate decreased E/I ratio. **(Ciii))** Relationship between percent change in the EPSC and IPSC following GlcN + TMG. Red circles indicate increased E/I and blue circles indicate decreased E/I ratio. **(Di)** Normalized group data showing average (±SEM) evoked mono-synaptic EPSP (filled circles) and di-synaptic IPSP (open circles) amplitude in control conditions and following GlcN + TMG wash on. **(Dii)** Representative compound EPSP and IPSP before (black) and after (blue) GlcN + TMG. (middle). **(Diii)** EPSP amplitude before (black) and after (blue) GlcN + TMG. Red horizontal bars represent the mean ± SEM. control: 12.3 ± 1.6 mV vs GlcN + TMG: 13.2 ± 1.9 mV ($p = 0.40$, paired t-test, n = 6 cells, 3 rats). (right) IPSP amplitude before (black) and after (blue) GlcN + TMG. Red horizontal bars represent the mean ± SEM. control: 7.8 ± 1.1 mV vs GlcN + TMG: 6.2 ± 0.9 mV ($p = 0.01$, paired t-test, n = 6 cells, 3 rats).

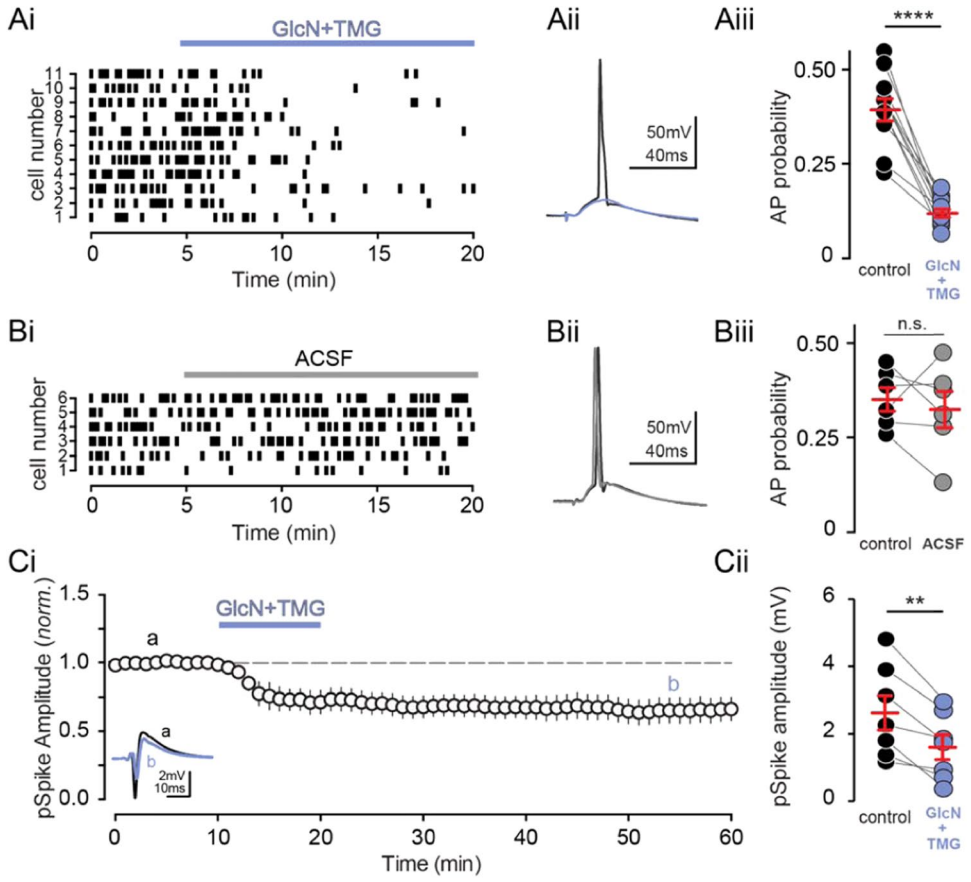

Figure 5. O-GlcNAcylation reduces CA1 action potential output. **(Ai)** Raster plot and **(Aii)** representative trace of synaptically-evoked APs before (black) and after GlcN + TMG (blue). **(Aiii)** AP probability before (black) and after (blue) GlcN + TMG. Red bars represent mean ± SE. control: 0.39 ± 0.03 vs. GlcN + TMG: 0.12 ± 0.01 ($p < 0.0001$, paired t-test, n = 11 cells, 6 rats). **(Bi)** Raster plot and **(Bii)** representative average of synaptically-evoked APs before (black) and after (grey) ACSF application as a negative control. **(Biii)** Quantification of AP probability before (black) and after (grey) ACSF. Red bars represent mean ± SE. control: 0.35 ± 0.03 vs. GlcN + TMG: 0.33 ± 0.05 ($p = 0.6$, paired t-test, n = 6 cells, 4 rats). **(Ci)** Normalized Group data showing pop-spike amplitude in baseline conditions and after GlcN + TMG (left). *inset:* representative trace showing pop spike before (black) and after (blue) GlcN + TMG. **(Cii)** pSpike amplitude before (black) and after (blue) GlcN + TMG. Red bars represent mean ± SEM. control: 2.64 ± 0.52 mV vs. GlcN + TMG: 1.61 ± 0.38 mV ($p = 0.004$, paired t-test, n = 7 slices, 3 rats).**$p < 0.01$, ****$p < 0.0001$.

Therefore, we next tested the possibility that O-GlcNAcylation decreases intrinsic excitability by modulating the active and passive properties of CA1 pyramidal cells. We used whole-cell current clamp recordings of CA1 pyramidal cells during hyperpolarizing and depolarizing current injections in the presence of pharmacological blockers of $GABA_A$Rs, AMPARs, and NMDARs, to isolate the cells from synaptic inputs (Fig. 6A). We found that O-GlcNAcylation caused a significant reduction in the input resistance (Fig. 6C, $p = 0.031$, paired t-test) when cells were isolated from the synaptic network, and a significant increase in rheobase, or the minimum current required to elicit a single action potential (Fig. 6D, $p = 0.036$, paired t-test). We also observed an increase in AP threshold (Fig. 6E, $p = 0.030$, paired t-test), but no difference in AP shape (Fig. 6F–H, AP amplitude: $p = 0.441$; AP rise: $p = 0.143$; AP half width: $p = 0.653$, paired t-test). Additionally, we found a small but significant decrease in the number of action potentials generated with higher current injection steps following GlcN + TMG application ($F_{O\text{-}GlcNAc}(1,8) = 5.81$, $p < 0.05$, two-way repeated measures ANOVA). These changes are consistent with a decrease in intrinsic excitability.

Collectively, our current and previously published data[18] suggest that both synaptic and intrinsic mechanisms contribute to a net decrease in CA1 pyramidal cell excitability, despite a larger O-GlcNAc-mediated depression of inhibitory versus excitatory transmission. Therefore, to distinguish the decreased intrinsic excitability from the synaptic depression at excitatory synapses, we repeated the pSpike recordings in GluA2 KO mice in which O-GlcNAc LTD at CA3-CA1 synapses will be absent (Fig. 7Ai,Aii). Interestingly, increasing O-GlcNAcylation depressed pSpike amplitude in both the wild-type and GluA2 KO mice (Fig. 7Aiii, control: $p < 0.01$ KO: $p < 0.01$, Sidak's multiple comparisons test), while the persistent depression (O-GlcNAc LTD) following GlcN + TMG wash-out was only observed in wild-type mice, as expected (Fig. 7Aiii, control: $p < 0.01$ KO: $p > 0.05$, Sidak's multiple comparison test). Thus, the early depression of the pSpike amplitude during GlcN + TMG application

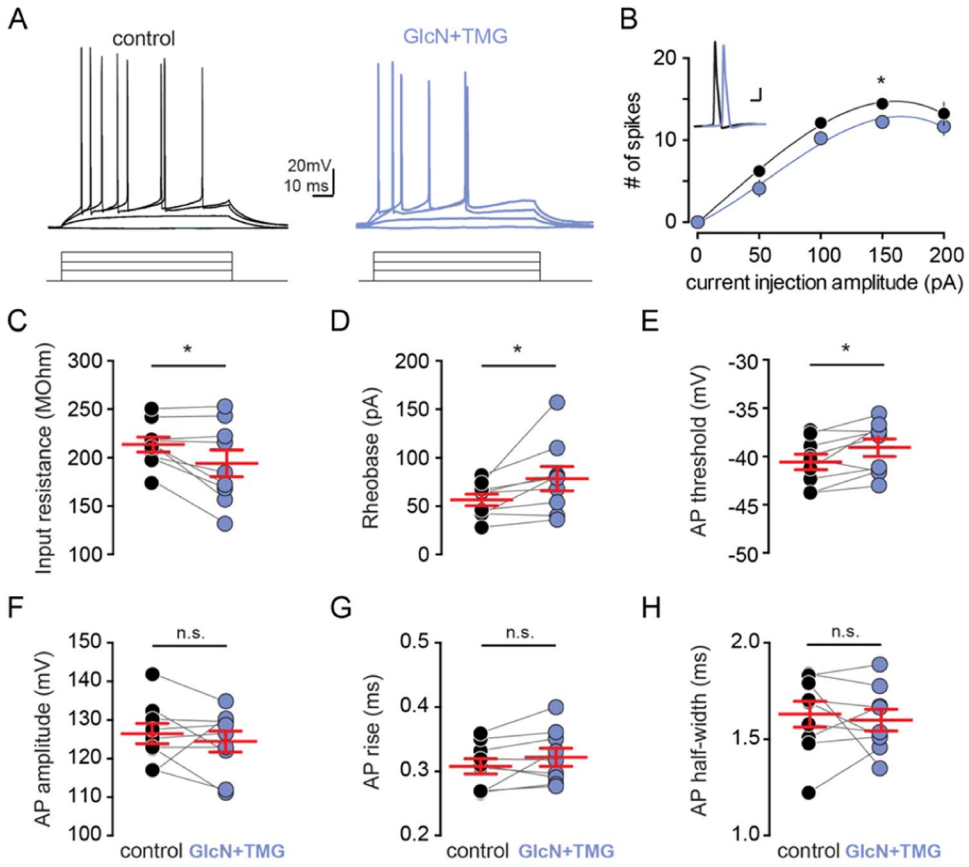

Figure 6. O-GlcNAcylation reduces intrinsic excitability of CA1 pyramidal cells. **(A)** Voltage responses to current injections (bottom, 800 ms, 20 pA steps) before (black) and after (blue) GlcN + TMG. **(B)** Number of spikes elicited by increasing current steps before (black) and after (blue) GlcN + TMG. Circles represent mean ± SEM. *Inset:* AP waveform before (black) and after (blue) GlcN + TMG. (scale bar: 20 mV, 10 ms). **(C)** Input resistance, **(D)** rheobase, **(E)** AP threshold, **(F)** AP amplitude, **(G)** AP rise, and **(H)** AP half-width before (black) and after (blue) GlcN + TMG. Red bars indicate mean ± SEM. Input resistance: 213.4 ± 7.7 MΩ (control) vs 194.1 ± 13.7 MΩ (GlcN + TMG) ($p = 0.031$, paired t-test). Rheobase: 56.7 ± 5.9 pA (control) vs 78.4 ± 12.5 pA (GlcN + TMG) ($p = 0.04$, paired t-test). AP threshold: −40.6 ± 0.8 mV (control) vs −39.1 ± 0.9 mV (GlcN + TMG) ($p = 0.030$, paired t-test). AP amplitude: 126.3 ± 2.6 mV(control) vs 124.3 ± 2.7 mV (GlcN + TMG) ($p = 0.44$, paired t-test). Rise: 0.31 ± 0.01 ms (control) vs 0.32 ± 0.01 ms (GlcN + TMG) ($p = 0.14$, paired t-test). AP half-width: 1.63 ± 0.07 ms(control) vs 1.59 ± 0.06 (GlcN + TMG) ($p = 0.653$, paired t-test, $n = 9$ cells, 2 rats). *$p < 0.05$.

is likely a consequence of decreasing CA1 pyramidal cell intrinsic excitability, while the persistent depression of excitability is a consequence of synaptic depression mediated by O-GlcNAc LTD.

Discussion

We provide, for the first time, empirical evidence of a role for protein O-GlcNAcylation in regulating synaptic inhibition in principal cells of the hippocampus. First, we show that acutely increasing O-GlcNAcylation reduces the frequency and magnitude of sIPSCs in CA1 pyramidal cells and dentate granule cells, and selectively decreases the amplitude of mIPSCs, suggesting a postsynaptic mechanism. The amplitude of evoked IPSCs onto CA1 pyramidal cells is similarly reduced, and the depression is long-lasting, suggesting a form of LTD induced by O-GlcNAc at GABAergic synapses. Second, in a hippocampal circuit with intact excitation and inhibition, an acute increase in O-GlcNAcylation has a variable effect on the E/I ratio, despite a greater effect on inhibition vs excitation. Finally, we show that O-GlcNAcylation modulates the final output of CA1 pyramidal cells by reducing the action potential probability through intrinsic and synaptic mechanisms. These results position protein O-GlcNAcylation as a potent regulator of both synaptic inhibition as well as excitation, as we reported previously[18,19].

While the effect of the analogous post translational modification, phosphorylation, on synaptic transmission has been extensively characterized, little is known about the role of O-GlcNAcylation on excitatory and inhibitory transmission. We have previously shown that acute increases in O-GlcNAcylation causes a GluA2 AMPAR subunit dependent long-term depression of excitatory transmission, O-GlcNAc LTD, in CA1 pyramidal cell dendritic field potentials and CA1 population spikes[18,19]. Here, we report that an acute increase in protein

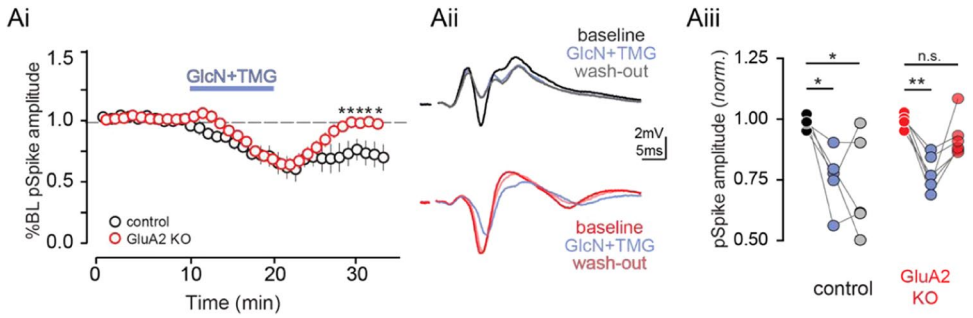

Figure 7. Increased O-GlcNAcylation reduces CA1 spike output. **(Ai)** Normalized group data showing pSpike amplitude in baseline conditions and after GlcN + TMG in control (black) and GluA2 KO (red) mice (*$p < 0.05$, two-way ANOVA with Sidak's multiple comparison test, n = 5 slices, 2 rats). **(Aii)** Representative averaged traces showing (top) pSpike amplitude before (black), after (blue) GlcN + TMG, and following wash-out (grey) in control mice and (bottom) pSpike amplitude before (red), after (blue) GlcN + TMG and following wash-out (pink) in GluA2 KO mice. **(Aiii)** Pop spike amplitude before (black), after (blue) GlcN + TMG and following wash-out (grey) in control mice (baseline vs. GlcN + TMG: $p < 0.05$; baseline vs. wash-out: $p < 0.05$, repeated measures one-way ANOVA with Sidak's multiple comparison's test, n = 5 slices, 2 rats) and pSpike amplitude before (red), after (blue) GlcN + TMG, and following wash-out (pink) in GluA2 KO mice (baseline vs. GlcN + TMG: $p < 0.01$; baseline vs. wash-out: $p > 0.05$, repeated measures one-way ANOVA with Sidak's multiple comparison's test, n = 5 slices, 2 rats). *$p < 0.05$, **$p < 0.01$.

O-GlcNAcylation similarly causes a depression of inhibition onto CA1 pyramidal cells and dentate granule cells. This includes a reduction in the amplitude but not frequency of mIPSCs onto hippocampal principal cells, suggesting a post-synaptic site of action. This reduction in inhibition could involve a number of mechanisms including internalization of $GABA_A$Rs, a change in the conductance of individual $GABA_A$Rs, or destabilization of scaffolding proteins that anchor $GABA_A$Rs to the membrane. Indeed, recent work[22] suggests the reduction in mEPSC amplitude following increased O-GlcNAcylation involves the endocytosis of GluA2 subunit containing AMPARs, which likely explains expression of the GluA2-dependent LTD we previously reported[19]. Additionally, phosphorylation of specific serine/threonine residues on $GABA_A$Rs modulates inhibitory transmission, an effect that includes a reduction in $GABA_A$R currents[9], which might also occur following increased O-GlcNAc.

Notably, phosphorylation alters inhibition in the brain in a kinase- and region-specific manner (for review, see[9]). Activation of PKA depresses synaptic $GABA_A$R function in CA1 pyramidal cells but not dentate gyrus granule cells (GCs), whereas PKC activation alters mini-IPSC amplitude in GCs alone[28]. O-GlcNAcylation, however, is uniquely positioned to turn down global inhibition in a non region-specific manner as only one enzyme, OGT, is known to catalyze its addition to proteins. While phosphorylation and O-GlcNAcylation on some proteins can occlude one another[29–33], other times they can act independently[19] or synergistically (for review, see[34]). Whether there is a negative or positive interplay between the effects of phosphorylation and O-GlcNAcylation on inhibition remains to be determined.

We show that acute increases in O-GlcNAcylation rapidly depress the di-synaptic IPSC while having a variable effect on the amplitude of the EPSC. This variability is likely explained by competing mechanisms including an O-GlcNAc mediated decrease in the inhibitory shunt and O-GlcNAc LTD at excitatory synapses. These changes are complex as indicated by the variable effect on the E/I ratio with some cells experiencing a significant increase and others a decrease such that a significant change in the averaged dataset is not observed. Despite this, there is a consistent reduction in the synaptically-evoked action potential probability in pyramidal cells. While subthreshold EPSPs can spatially and temporally summate to generate APs, the efficacy of EPSP to spike coupling is thought to depend on several factors including IPSP magnitude and timing[35], as well as passive and active properties of the post-synaptic neuron[36]. Interestingly, (i) individual pyramidal cells vary widely in their threshold afferent stimulation required for spiking, but this threshold is controlled by the magnitude of the EPSC and not the amplitude or timing of inhibition[37]; and (ii) increasing O-GlcNAcylation leads to a depression of field EPSPs in area CA1, likely owing to an internalization of GluA2 containing AMPARs[18,22]. Thus, it stands to reason that the decrease in AP probability could stem from a concomitant depression of the CA3-CA1 EPSC. We found that O-GlcNAcylation not only reduces the AMPAR mediated dendritic depolarization[19], but also changes the intrinsic properties of CA1 neurons, making it harder for the cell to spike. This change in intrinsic properties following an increase in O-GlcNAc we report here in rats is consistent with recently published work by Hwang & Rhim[22] showing a reduction in depolarizing voltage-gated sodium channel currents and an increase in hyperpolarizing voltage-gated potassium currents in recordings from mice. The slightly larger effect observed by Hwang & Rhim compared to what we report here is likely due to a species difference, as we observed a larger decrease in CA1 pyrmaidal cell excitability following GlcN + TMG application in our previous report in mice compared to rats[18]. We have also previously reported a reduction in basal spontaneous spiking activity in area CA3 of hippocampus following increased O-GlcNAc[18], further supporting a suppressive effect of O-GlcNAcylation on neuronal output. Notably, this finding is contrary to studies using genetic strategies to increase O-GlcNAcylation[20], which reported no changes in intrinsic excitability, or mini-EPSCs and -IPSCs following heterozygous loss of function mutation of OGA, whose protein product catalyzes the removal of O-GlcNAc from proteins. The conflicting results

are mostly likely due to differential effects of acute versus chronic upregulation in protein O-GlcNAcylation, as chronic changes can produce compensatory mechanisms to maintain synaptic function.

Studying the effect of acute, moment-to-moment changes in global O-GlcNAc levels on synaptic transmission likely reflects the impact of metabolically driven changes in O-GlcNAcylation occurring *in vivo* under both physiological and pathophysiological conditions. The OGT substrate UDP-GlcNAc is produced by the flux of glucose through the hexosamine biosynthetic pathway, which incorporates nucleotides, fatty acids, and amino acids. As such, O-GlcNAcylation is positioned to operate as a nutrient sensor (for review, see[38]). For instance, fasting promotes energy conservation via the upregulation of OGT and O-GlcNAc and its effect on the activity of hypothalamic neurons[17]. Conversely, chronic elevation of glucose can also increase O-GlcNAcylation of certain targets, contributing to cardiac and neuronal pathophysiology[39]. Additionally, O-GlcNAcylation plays a crucial role in pathological states such as diabetes[39,40] where its elevation can contribute to disease pathogenesis, in epilepsy where increasing O-GlcNAc is protective[18,41], and in neurodegeneration[42–49], where increasing O-GlcNAc can decrease pathological accumulation of phosphorylated tau or α-synuclein. Collectively, studies published by us and others suggest that maintaining proper balance in O-GlcNAcylation is critical to maintaining normal hippocampal function, as too much or too little O-GlcNAc has been linked to deficits in learning and memory[19,20,42]. Revealing the complex changes in neuronal and synaptic function induced by alterations in O-GlcNAcylation in non-pathological and pathological states will require further investigation.

Materials and methods

All experimental procedures were approved by the University of Alabama at Birmingham Institutional Animal Care and Use Committee and follow the National Institutes of Health experimental guidelines.

Hippocampal slice preparation. Male and female Sprague Dawley rats (age 4–8 weeks; Charles River Laboratories) or male and female mice (age 4–12 weeks, GluA2 KO, Jax Labs #002913) were anesthetized with isoflurane, rapidly decapitated, and brains removed; 400μm (rats) or 350 μm (mice) coronal slices from dorsal hippocampus were prepared on a VT1000P vibratome (Leica Biosystems) in oxygenated (95%O_2/5%CO_2) ice-cold, high sucrose cutting solution (in mM as follows: 85.0 NaCl, 2.5 KCl, 4.0 $MgSO_4$, 0.5 $CaCl_2$, 1.25 $NaPO_4$, 25.0 glucose, 75.0 sucrose). After cutting, slices were held at room temperature for 1 to 5 hr in a submersion chamber with continuously oxygenated standard ACSF (in mM as follows: 119.0 NaCl, 2.5 KCl, 1.3 $MgSO_4$, 2.5 $CaCl_2$, 1.0 NaH_2PO_4, 26.0 $NaHCO_3$, 11.0 glucose) with 2 mM kynurenic acid to better preserve slice health.

Electrophysiology. All recordings were performed in a submersion chamber with continuous perfusion of oxygenated standard ACSF. The blind patch technique was used to acquire whole-cell recordings from CA1 pyramidal neurons and dentate granule cells (GCs). Neuronal activity was recorded using an Axopatch 200B amplifier and pClamp10 acquisition software (Molecular Devices, Sunnyvale, CA). Signals were filtered at 5 kHz and digitized at 10 kHz (Digidata 1440). Patch pipettes (BF150-086 or BF150-110; Sutter Instruments, Novato, CA) were pulled on a Sutter P-97 (Sutter Instruments, Novato, CA) horizontal puller to a resistance between 2–6 MΩ. Spontaneous inhibitory postsynaptic currents (sIPSCs) were pharmacologically isolated with bath perfusion of DNQX (10μM; Sigma) and DL-AP5 (50μM; Tocris) or R-CPP (5 μM; Abcam). Purity of $GABA_AR$ currents was verified with perfusion of picrotoxin (50μM; Sigma) following experimental recording. Spontaneous and miniature IPSCs were recorded using CsCl internal solution (in mM: 140.0 CsCl, 10.0 EGTA, 5.0 $MgCl_2$, 2.0 Na-ATP, 0.3 Na-GTP, 10.0 HEPES; $E_{Cl} = 0$ mV). Evoked $GABA_AR$ currents were recorded using Cs-gluconate internal solution (in mM: 100.0 Cs-gluconate, 0.6 EGTA, 5.0 $MgCl_2$, 2.0 Na-ATP, 0.3 Na-GTP, 40.0 HEPES; $E_{Cl} = -61.5$ mV) with a twisted nichrome wire bipolar electrode positioned in stratum radiatum (100μs, 0.1 Hz). Whole-cell current clamp recordings from CA1 pyramidal neurons were carried out using K-gluconate internal solution (in mM: 120.0 K-gluconate, 0.6 EGTA, 5.0 MgCl2, 2.0 Na-ATP, 0.3 Na-GTP, 20.0 HEPES; ECl = −61.5 mV). All cells were dialized for 3–7 min prior to the beginning of experimental recordings. Stability of series resistance was verified using post-hoc scaling of averaged waveforms before and after pharmacologicaly increasing O-GlcNAcylation. pSpikes in the CA1 cell body layer were evoked by stimulating Schaffer collaterals with pairs of pulses (0.1 Hz, 100 μs duration at 50 ms interval) in stratum radiatum with a twisted nichrome wire bipolar electrode and recorded with a glass pipet filled with aCSF placed nearby in stratum pyramidale.

Modulation of O-GlcNAc levels. As previously described[18,19] O-GlcNAcylation was acutely increased via bath application of glucosamine (GlcN, 5 mM; Sigma) alone or in combination with the selective OGA inhibitor TMG (1 μM; Chem Molecules), the most potent OGA inhibitor ($Ki = 21$ nM; human OGA) currently available[46,50]. GlcN and TMG were used in combination to ensure robust and lasting increases in protein O-GlcNAc levels. In some experiments, we tested whether applying the HBP substrate GlcN alone was sufficient to modulate inhibitory transmission, as this approach more closely recapitulates the endogenous regulation of cellular O-GlcNAcylation.

Experimental design and statistical analysis. Recordings were analyzed using Clampfit 10.6. Outliers were determined as per outlier test in GraphPad Prism 8.1.0, La Jolla, CA, and excluded. For two-group comparisons, statistical significance was determined by two-tailed paired or unpaired Student's t-tests (parametric), or Wilcoxon matched-pairs signed rank test (non-parametric, paired). Multi-groups were analyzed using repeated measure one-way ANOVA with Sidak correction (parametric) or repeated measure two-way ANOVA with Sidak's test (non-parametric) (GraphPad Prism 8.1.0, La Jolla, CA). Data are displayed as mean ± SEM and p values less than 0.05 were considered statistically significant.

Data availability

The datasets generated during and/or analysed during the current study are available from the corresponding author on reasonable request

Received: 20 October 2019; Accepted: 2 March 2020;
Published online: 04 May 2020

References

1. Farrant, M. & Nusser, Z. Variations on an inhibitory theme: phasic and tonic activation of GABA(A) receptors. *Nat. Rev. Neurosci.* **6**, 215–229 (2005).
2. Fernandez, F. *et al*. Pharmacotherapy for cognitive impairment in a mouse model of Down syndrome. *Nat. Neurosci.* **10**, 411–413 (2007).
3. Kehrer, C., Maziashvili, N., Dugladze, T. & Gloveli, T. Altered Excitatory-Inhibitory Balance in the NMDA-Hypofunction Model of Schizophrenia. *Front. Mol. Neurosci.* **1**, 6 (2008).
4. Gogolla, N. *et al*. Common circuit defect of excitatory-inhibitory balance in mouse models of autism. *J. Neurodev. Disord.* **1**, 172–181 (2009).
5. Roberson, E. D. *et al*. Amyloid-β/Fyn-induced synaptic, network, and cognitive impairments depend on tau levels in multiple mouse models of Alzheimer's disease. *J. Neurosci.* **31**, 700–711 (2011).
6. Saliba, R. S., Michels, G., Jacob, T. C., Pangalos, M. N. & Moss, S. J. Activity-dependent ubiquitination of GABA(A) receptors regulates their accumulation at synaptic sites. *J. Neurosci.* **27**, 13341–13351 (2007).
7. Keller, C. A. *et al*. The gamma2 subunit of GABA(A) receptors is a substrate for palmitoylation by GODZ. *J. Neurosci.* **24**, 5881–5891 (2004).
8. Rathenberg, J., Kittler, J. T. & Moss, S. J. Palmitoylation regulates the clustering and cell surface stability of GABAA receptors. *Mol. Cell. Neurosci.* **26**, 251–257 (2004).
9. Nakamura, Y., Darnieder, L. M., Deeb, T. Z. & Moss, S. J. Regulation of GABAARs by phosphorylation. *Adv. Pharmacol.* **72**, 97–146 (2015).
10. Shafi, R. *et al*. The O-GlcNAc transferase gene resides on the X chromosome and is essential for embryonic stem cell viability and mouse ontogeny. *Proc. Natl. Acad. Sci. USA* **97**, 5735–5739 (2000).
11. Keembiyehetty, C. *et al*. Conditional knock-out reveals a requirement for O-linked N-Acetylglucosaminase (O-GlcNAcase) in metabolic homeostasis. *J. Biol. Chem.* **290**, 7097–7113 (2015).
12. Yang, X. & Qian, K. Protein O-GlcNAcylation: emerging mechanisms and functions. *Nat. Rev. Mol. Cell Biol.* **18**, 452–465 (2017).
13. Kreppel, L. K., Blomberg, M. A. & Hart, G. W. Dynamic glycosylation of nuclear and cytosolic proteins. Cloning and characterization of a unique O-GlcNAc transferase with multiple tetratricopeptide repeats. *J. Biol. Chem.* **272**, 9308–9315 (1997).
14. Liu, K. *et al*. Accumulation of protein O-GlcNAc modification inhibits proteasomes in the brain and coincides with neuronal apoptosis in brain areas with high O-GlcNAc metabolism. *J. Neurochem.* **89**, 1044–1055 (2004).
15. Trinidad, J. C. *et al*. Global identification and characterization of both O-GlcNAcylation and phosphorylation at the murine synapse. *Mol. Cell Proteomics* **11**, 215–229 (2012).
16. Lagerlöf, O., Hart, G. W. & Huganir, R. L. O-GlcNAc transferase regulates excitatory synapse maturity. *Proc. Natl. Acad. Sci. USA* **114**, 1684–1689 (2017).
17. Ruan, H.-B. *et al*. O-GlcNAc transferase enables AgRP neurons to suppress browning of white fat. *Cell* **159**, 306–317 (2014).
18. Stewart, L. T. *et al*. Acute Increases in Protein O-GlcNAcylation Dampen Epileptiform Activity in Hippocampus. *J. Neurosci.* **37**, 8207–8215 (2017).
19. Taylor, E. W. *et al*. O-GlcNAcylation of AMPA receptor GluA2 is associated with a novel form of long-term depression at hippocampal synapses. *J. Neurosci.* **34**, 10–21 (2014).
20. Yang, Y. R. *et al*. Memory and synaptic plasticity are impaired by dysregulated hippocampal O-GlcNAcylation. *Sci. Rep.* **7**, 44921 (2017).
21. Hwang, H. & Rhim, H. Functional significance of O-GlcNAc modification in regulating neuronal properties. *Pharmacol. Res.* **129**, 295–307 (2018).
22. Hwang, H. & Rhim, H. Acutely elevated O-GlcNAcylation suppresses hippocampal activity by modulating both intrinsic and synaptic excitability factors. *Sci. Rep.* **9**, 7287 (2019).
23. Lagerlöf, O. *et al*. The nutrient sensor OGT in PVN neurons regulates feeding. *Science* **351**, 1293–1296 (2016).
24. McDonald, B. J. & Moss, S. J. Conserved phosphorylation of the intracellular domains of GABA(A) receptor beta2 and beta3 subunits by cAMP-dependent protein kinase, cGMP-dependent protein kinase protein kinase C and Ca2+/calmodulin type II-dependent protein kinase. *Neuropharmacology* **36**, 1377–1385 (1997).
25. Vithlani, M., Terunuma, M. & Moss, S. J. The dynamic modulation of GABA(A) receptor trafficking and its role in regulating the plasticity of inhibitory synapses. *Physiol. Rev.* **91**, 1009–1022 (2011).
26. Kavalali, E. T. The mechanisms and functions of spontaneous neurotransmitter release. *Nat. Rev. Neurosci.* **16**, 5–16 (2015).
27. Mitchel, S. J. & Silver, R. A. Shunting inhibition modulates neuronal gain during synaptic excitation. *Neuron* **38**, 433–45 (2003).
28. Poisbeau, P., Cheney, M. C., Browning, M. D. & Mody, I. Modulation of synaptic GABAA receptor function by PKA and PKC in adult hippocampal neurons. *J. Neurosci.* **19**, 674–683 (1999).
29. Liu, F., Iqbal, K., Grundke-Iqbal, I., Hart, G. W. & Gong, C.-X. O-GlcNAcylation regulates phosphorylation of tau: a mechanism involved in Alzheimer's disease. *Proc. Natl. Acad. Sci. USA* **101**, 10804–10809 (2004).
30. Chou, T. Y., Hart, G. W. & Dang, C. V. c-Myc is glycosylated at threonine 58, a known phosphorylation site and a mutational hot spot in lymphomas. *J. Biol. Chem.* **270**, 18961–18965 (1995).
31. Cheng, X., Cole, R. N., Zaia, J. & Hart, G. W. Alternative O-Glycosylation/O-Phosphorylation of the Murine Estrogen Receptor β. *Biochemistry* **39**, 11609–11620 (2000).
32. Griffith, L. S. & Schmitz, B. O-linked N-acetylglucosamine levels in cerebellar neurons respond reciprocally to pertubations of phosphorylation. *Eur. J. Biochem.* **262**, 824–831 (1999).
33. Dias, W. B., Cheung, W. D., Wang, Z. & Hart, G. W. Regulation of calcium/calmodulin-dependent kinase IV by O-GlcNAc modification. *J. Biol. Chem.* **284**, 21327–21337 (2009).
34. Zeidan, Q. & Hart, G. W. The intersections between O-GlcNAcylation and phosphorylation: implications for multiple signaling pathways. *J. Cell Sci.* **123**, 13–22 (2010).
35. Pouille, F. & Scanziani, M. Enforcement of temporal fidelity in pyramidal cells by somatic feed-forward inhibition. *Science* **293**, 1159–1163 (2001).
36. Magee, J. C. Dendritic integration of excitatory synaptic input. *Nat. Rev. Neurosci.* **1**, 181–190 (2000).
37. Pouille, F., Marin-Burgin, A., Adesnik, H., Atallah, B. V. & Scanziani, M. Input normalization by global feedforward inhibition expands cortical dynamic range. *Nat. Neurosci.* **12**, 1577–1585 (2009).
38. Lagerlöf, O. O-GlcNAc cycling in the developing, adult and geriatric brain. *J Bioenerg Biomembr* **50**, 241–261 (2018).

39. Erickson, J. R. *et al*. Diabetic hyperglycaemia activates CaMKII and arrhythmias by O-linked glycosylation. *Nature* **502**, 372–376 (2013).
40. Vaidyanathan, K. & Wells, L. Multiple tissue-specific roles for the O-GlcNAc post-translational modification in the induction of and complications arising from type II diabetes. *J. Biol. Chem.* **289**, 34466–34471 (2014).
41. Sánchez, R. G. *et al*. Human and rodent temporal lobe epilepsy is characterized by changes in O-GlcNAc homeostasis that can be reversed to dampen epileptiform activity. *Neurobiol. Dis.* **124**, 531–543 (2019).
42. Wang, A. C., Jensen, E. H., Rexach, J. E., Vinters, H. V. & Hsieh-Wilson, L. C. Loss of O-GlcNAc glycosylation in forebrain excitatory neurons induces neurodegeneration. *Proc. Natl. Acad. Sci. USA* **113**, 15120–15125 (2016).
43. Yuzwa, S. A., Cheung, A. H., Okon, M., McIntosh, L. P. & Vocadlo, D. J. O-GlcNAc modification of tau directly inhibits its aggregation without perturbing the conformational properties of tau monomers. *J. Mol. Biol.* **426**, 1736–1752 (2014).
44. Yuzwa, S. A. *et al*. Pharmacological inhibition of O-GlcNAcase (OGA) prevents cognitive decline and amyloid plaque formation in bigenic tau/APP mutant mice. *Mol. Neurodegener.* **9**, 42 (2014).
45. Yuzwa, S. A. *et al*. Increasing O-GlcNAc slows neurodegeneration and stabilizes tau against aggregation. *Nat. Chem. Biol.* **8**, 393–399 (2012).
46. Yuzwa, S. A. *et al*. A potent mechanism-inspired O-GlcNAcase inhibitor that blocks phosphorylation of tau *in vivo*. *Nat. Chem. Biol.* **4**, 483–490 (2008).
47. Zhu, Y., Shan, X., Yuzwa, S. A. & Vocadlo, D. J. The emerging link between O-GlcNAc and Alzheimer disease. *J. Biol. Chem.* **289**, 34472–34481 (2014).
48. Yuzwa, S. A. & Vocadlo, D. J. O-GlcNAc and neurodegeneration: biochemical mechanisms and potential roles in Alzheimer's disease and beyond. *Chem. Soc. Rev.* **43**, 6839–6858 (2014).
49. Levine, P. M. *et al*. α-Synuclein O-GlcNAcylation alters aggregation and toxicity, revealing certain residues as potential inhibitors of Parkinson's disease. *Proc. Natl. Acad. Sci. USA* **116**, 1511–1519 (2019).
50. Macauley, M. S., Whitworth, G. E., Debowski, A. W., Chin, D. & Vocadlo, D. J. O-GlcNAcase uses substrate-assisted catalysis: kinetic analysis and development of highly selective mechanism-inspired inhibitors. *J. Biol. Chem.* **280**, 25313–22 (2005).

Acknowledgements

This research was supported by NIH NINDS R01NS076312 and R21NS11945 to LLM and JCC, 1F31NS095568 to LTS, and an Alabama State funded Graduate Research Scholars Program Fellowship (GRSP) to KA. We would like to thank former and current members of the McMahon lab for valuable discussions during the development of this manuscript. This manuscript is hosted as a preprint on biorxiv at https://doi.org/10.1101/672055.

Author contributions

L.T.S., K.A., and L.L.M. designed the experiments; L.T.S. and K.A. conducted experiments; L.T.S., K.A., and L.L.M. analyzed data; L.T.S., K.A., J.C.C., and L.L.M. wrote and revised the manuscript.

Competing interests

The authors declare no competing interests.

Additional information

Correspondence and requests for materials should be addressed to L.L.M.

Reprints and permissions information is available at www.nature.com/reprints.

Publisher's note Springer Nature remains neutral with regard to jurisdictional claims in published maps and institutional affiliations.